

Cortical Up State Activity Is Enhanced After Seizures: A Quantitative Analysis

Richard C. Gerkin,*† Roger L. Clem,†‡ Sonal Shruti,†‡ Robert E. Kass,‡§ and Alison L. Barth†‡

Abstract: In the neocortex, neurons participate in epochs of elevated activity, or Up states, during periods of quiescent wakefulness, slow-wave sleep, and general anesthesia. The regulation of firing during and between Up states is of great interest because it can reflect the underlying connectivity and excitability of neurons within the network. Automated analysis of the onset and characteristics of Up state firing across different experiments and conditions requires a robust and accurate method for Up state detection. Using measurements of membrane potential mean and variance calculated from whole-cell recordings of neurons from control and postseizure tissue, the authors have developed such a method. This quantitative and automated method is independent of cell- or condition-dependent variability in underlying noise or tonic firing activity. Using this approach, the authors show that Up state frequency and firing rates are significantly increased in layer 2/3 neocortical neurons 24 hours after chemoconvulsant-induced seizure. Down states in postseizure tissue show greater membrane-potential variance characterized by increased synaptic activity. Previously, the authors have found that postseizure increase in excitability is linked to a gain-of-function in BK channels, and blocking BK channels *in vitro* and *in vivo* can decrease excitability and eliminate seizures. Thus, the authors also assessed the effect of BK-channel antagonists on Up state properties in control and postseizure neurons. These data establish a robust and broadly applicable algorithm for Up state detection and analysis, provide a quantitative description of how prior seizures increase spontaneous firing activity in cortical networks, and show how BK-channel antagonists reduce this abnormal activity.

Key Words: epilepsy, seizure, Up state, BK channels, classification

(*J Clin Neurophysiol* 2010;27: 425–432)

Synchronized activity of neuronal populations has been detected in the neocortex during both wakefulness and sleep (reviewed by Haider and McCormick, 2009). This activity is characterized by bistable periods of firing, or Up states interrupted by quiescent periods, or Down states. Up state activity results from recurrent excitation within neocortical networks and is readily observed both *in vivo* (Metherate and Ashe, 1993; Petersen et al., 2003; Steriade et al., 1993) and *in vitro* (Echevarria and Albus, 2000; Johnson and Buonomano, 2007; Sanchez-Vives and McCormick, 2000; Shu et al., 2003).

Although Up states are observed in healthy neocortex, changes in their frequency and duration may be a hallmark of abnormal brain function. Synchronized neural activity can serve as a substrate for

pathologic transformations of network output; for example, synchronized sensory visual input can induce seizures in susceptible individuals (Takada et al., 1999), and the slow oscillation during sleep facilitates a transition to epileptic seizures (Beenhakker and Huguenard, 2009; Steriade and Amzica, 2003). Recurrent network activity also underlies consolidation of maladaptive synaptic connections, facilitating the emergence of future seizures (Abegg et al., 2004; Bains et al., 1999; Kadam, et al., 2010; Shao and Dudek, 2004; Sutula et al., 1988).

Although some forms of intractable seizures localize to the hippocampus and have been well-studied experimentally, the neocortex is a common source of seizure initiation, especially in pediatric populations (Jensen, 2009). Indeed, the neocortex is a “minimal substrate” for seizure initiation (Steriade and Amzica, 2003). This brain area shows dense interconnectivity, especially within layer 2/3 neurons, which can propagate synchronized activity (Chagnac-Amitai and Connors, 1989; Sanchez-Vives and McCormick, 2000; Tsau et al., 1999). In addition, experimentally induced seizures robustly activate layer 2/3 neurons in rodent models as visualized by immediate-early gene expression (Willoughby et al., 1995). Here, we evaluate how prior seizures alter the network activity of layer 2/3 neocortical neurons, using whole-cell patch clamp recordings in acute brain slices.

Spontaneous firing activity of layer 2/3 neurons from control and postseizure mice was examined, with a particular focus on Up state characteristics. Because quantitative analysis of state-dependent firing output requires accurate determination of state transitions, we developed a robust algorithm for unsupervised detection of Up and Down states. This method bears similarities to other methods that have been described (Mukovski et al., 2006; Seamari et al., 2007) but is entirely unsupervised and nearly parameter free. We use this method to evaluate seizure-induced changes in Up and Down state characteristics *in vitro*. A quantitative analysis of state characteristics during spontaneous activity can inform understanding of both alterations in network connectivity and the specific ionic conductances controlling this slow oscillation under both normal and pathologic conditions.

Although short-term patterned stimulation can induce a long-term reduction in Up state frequency and Up state firing rate (Johnson and Buonomano, 2007), previous studies have not examined longer term transformations in firing output. Our analysis of Up state properties 24 hours after chemoconvulsant-induced seizures shows that both Up state frequency and Up state firing rate are increased compared with age-matched controls, while Up state duration is unaltered. Increased overall firing rates were accompanied by increases both in membrane potential variance as well as increased synaptic drive during the Down state. Application of the BK-channel antagonists, iberiotoxin or paxilline, reduced Up state firing activity but not Up state frequency, indicating that these features can be dissociated. The effect of BK-channel antagonists was present in control but was more pronounced in neurons from postseizure tissue. These results will help generate specific hypotheses about how seizure-dependent changes in neuronal function can act in antihomostatic ways to determine the emergent properties of neuronal network activity.

From the *Center for Neuroscience at the University of Pittsburgh; and †Center for the Neural Basis of Cognition, ‡Department of Biological Sciences, and §Department of Statistics, Carnegie Mellon University, Pittsburgh, Pennsylvania, U.S.A.

Supported by an IGERT award from NSF (to R.C.G.), a Milken Family Foundation Translational Research Award, and start-up funds from Carnegie Mellon University (to A.L.B.).

Address correspondence and reprint requests to Richard C. Gerkin and Alison L. Barth, Center for the Neural Basis of Cognition, Carnegie Mellon University, Pittsburgh, PA 15213, U.S.A.; e-mail: barth@cmu.edu.

Copyright © 2010 by the American Clinical Neurophysiology Society
ISSN: 0736-0258/10/2706-0425

MATERIALS AND METHODS

Animal Handling and Seizure Induction

C57/Bl6 mice were injected intraperitoneally at P13–P15 with 2 mg/kg picrotoxin. This treatment induced tonic-clonic seizures (80% of animals); only animals experiencing such seizures were used for analysis. Animals seized for approximately 20–40 minutes after injection. Picrotoxin injection did not subsequently produce spontaneous seizures, and 24 hours after the initial event, animals were behaviorally indistinguishable from control littermates, which served as electrophysiological controls. Animals were killed for electrophysiology 24 hours after treatment, between P13 and P15 (mean control: 14.2 and postseizure: 14.4 days).

Preparation of Brain Slices

Animals were anesthetized with isoflurane, decapitated, and their brains quickly removed. Coronal slices (400 μm) were prepared in ice-cold artificial cerebrospinal fluid (ACSF) saturated with 95% O₂–5% CO₂ containing (in mM): 119 NaCl, 2.5 KCl, 1.0 NaH₂PO₄, 1.3 MgCl₂, 2.5 CaCl₂, 26.2 NaHCO₃, and 11 glucose. After preparation of slices, tissue was maintained at room temperature in this solution.

Electrophysiology

Layer 2/3 pyramidal neurons in the barrel cortex were targeted for whole-cell recording. Sixteen animals were used for the seizure condition and 13 for the control condition. Typically, each cell was recorded from a separate brain slice. In all analysis, *n* refers to the number of cells (Current clamp—control: 35, postseizure: 33; Voltage clamp—control: 18, postseizure: 15) or the number of Up states (Current clamp—control: 278, postseizure: 352; Voltage clamp—control: 157, postseizure: 100) or Down states (control: 313; postseizure: 385).

Experiments were performed at room temperature in a modified ACSF (Maffei et al., 2004) with a physiologic calcium concentration (Fishman, 1992) to facilitate spontaneous activity containing (in mM): 0.5 MgCl₂, 1 CaCl₂, 119 NaCl, 2.5 KCl, 1.0 NaH₂PO₄, 26.2 NaHCO₃, and 11 glucose. The patch pipette contained a solution composed of (in mM): 125 K-gluconate, 10 HEPES, 2 KCl, 4 Mg-ATP, 0.25 Na-GTP, 0.05 Alexa-568. Pyramidal cell identity was confirmed *post hoc* by morphology and dendritic arborization and by the presence of dendritic spines under fluorescence microscopy. Neurons were held under current clamp with a steady-state holding current to depolarize neurons to a target membrane potential of –50 mV to normalize the ionic driving forces across neurons (Fig. 1A). Signals were acquired using a Multi-clamp 700B amplifier (Axon Instruments) and digitized at 10 kHz using a PCI-6036 A/D board (National Instruments). Data were acquired and analyzed using custom functions (written by R.C.G.) for Igor Pro (Wavemetrics, Lake Oswego, OR).

Identification of Up and Down states

A hallmark of network bistability is that Up states are characterized by an enhancement in the amplitude and/or rate of synaptic input compared with the Down state, and that both the membrane potential and its variability are increased (Shu et al., 2003; Zou et al., 2005). The algorithm developed here to detect transitions between Up and Down states exploits this by continuously estimating the mean and variance of the membrane potential and using these estimates to establish a threshold in a two-dimensional space that marks statistically significant changes in both quantities.

Determining what constitutes a significant change in membrane potential is challenging because the statistics that govern membrane potential time series during the Down state are not homogenous across time, cells, and contexts (Figs. 1B and 1D). For a threshold method to be consistent and robust, the membrane potential signal must be transformed to a homogeneous, stationary time

series. This transformation is achieved by expressing the membrane potential during the Down state as:

$$Y_t = \mu_t + \sigma_t W_t \tag{1}$$

The membrane potential Y_t is determined by the underlying mean μ_t , standard deviation σ_t , and a homogeneous, stationary, zero mean, unit variance noise term W_t . After applying the transformation $Y \rightarrow W$ (Fig. 1C), observation of a fixed threshold crossing, $\hat{w}_t > Q$ (Fig. 1F), would identify moments when the observed value \hat{w}_t was unlikely given the unit normal distribution of \hat{w} . Such a crossing would either be (a) a chance occurrence (false positive), or (b) an indication that the membrane potential was dictated by a new state, the Up state. To eliminate fast time-scale correlations and ensure that W_t during the Down state satisfies the above criteria, the recorded signal was decimated using bins with a width of the membrane time constant (~10 milliseconds), to generate a working signal y .

Computation of Mean and Variance

For each time point t , estimates are made for both the mean $\hat{\mu}_t$ and variance $\hat{\sigma}_t^2$ that instantaneously describe the membrane potential at that time, using an exponential filter, the simplest linear recursive filter:

$$\hat{\mu}_t = \hat{\mu}_{t-1} + y'_t/T \tag{2}$$

where $T = 1$ second and the initial estimate $\hat{\mu}_0$ is set equal to y_0 . The membrane potential variance estimate $\hat{\sigma}_t^2$ is computed with an analogous update equation. To ensure that this variance estimate was independent of trends in the data that might be on the order of T , $\hat{\sigma}_t^2$ was computed based on the time series y' , given by

$$y'_t = (y_t - y_{t-1})/\sqrt{2} \tag{3}$$

Using y' (Fig. 1D) obviates the need for a computational intensive detrending step. Because variance can be expressed as a summation, the same kind of recursive exponential filter can be used to estimate the variance over a recent period of time:

$$\hat{\sigma}_t^2 = \hat{\sigma}_{t-1}^2 + (y'_t - \hat{\mu}_t)^2/T \quad \hat{\mu}'_t = \hat{\mu}'_{t-1} + y'_t/T \tag{4, 5}$$

Finally, $\hat{\sigma}_t^2$ is equal to $\hat{\sigma}_t'^2$, reducing the actual number of estimation steps from 4 to 3. To identify states, a state variable S is initialized to zero. At every time step in $y(t)$, the estimates $(\hat{\mu}_t, \hat{\sigma}_t^2)$ and $(\hat{\mu}'_t, \hat{\sigma}_t'^2)$ are computed as above, as well as:

$$\hat{w}_t = (y_t - \hat{\mu}_t)/\hat{\sigma}_t \quad \hat{w}'_t = (y'_t - \hat{\mu}'_t)/\hat{\sigma}'_t \tag{6, 7}$$

which is the solution of Eq. 1 for W (Fig. 1C, and analogously for W' , Fig. 1E). The threshold for transition from a Down state to an Up state is given by a single parameter, Q , which is a constant = 2. When both \hat{w}_t and \hat{w}'_t exceed Q , the computation of $(\hat{\mu}_t, \hat{\sigma}_t^2)$ and $(\hat{\mu}'_t, \hat{\sigma}_t'^2)$ is suspended, and S is set to 1 (Figs. 1F and 1G). For every successive sample y_t , the inequalities are examined again. If both are no longer satisfied, S is set to 0 and the updating of $(\hat{\mu}_t, \hat{\sigma}_t^2)$ and $(\hat{\mu}'_t, \hat{\sigma}_t'^2)$ resumes. Otherwise, S remains equal to 1. Thus, the resultant time series $S(t)$ is equal to 1 when the evidence for an Up state exceeds a threshold level Q , and 0 otherwise. To consolidate 1-dense regions into Up states, and 0-dense regions into Down states, $S(t)$ is median smoothed using a window of width $T_{\text{smooth}} = 1$ second. Contiguous segments of the time series after this smoothing which remain equal to 1 are then classified as Up states. The entire algorithm can be implemented online with the exception of the final consolidation step, which improves accuracy (using a subjective inspection of the signal as the ground truth).

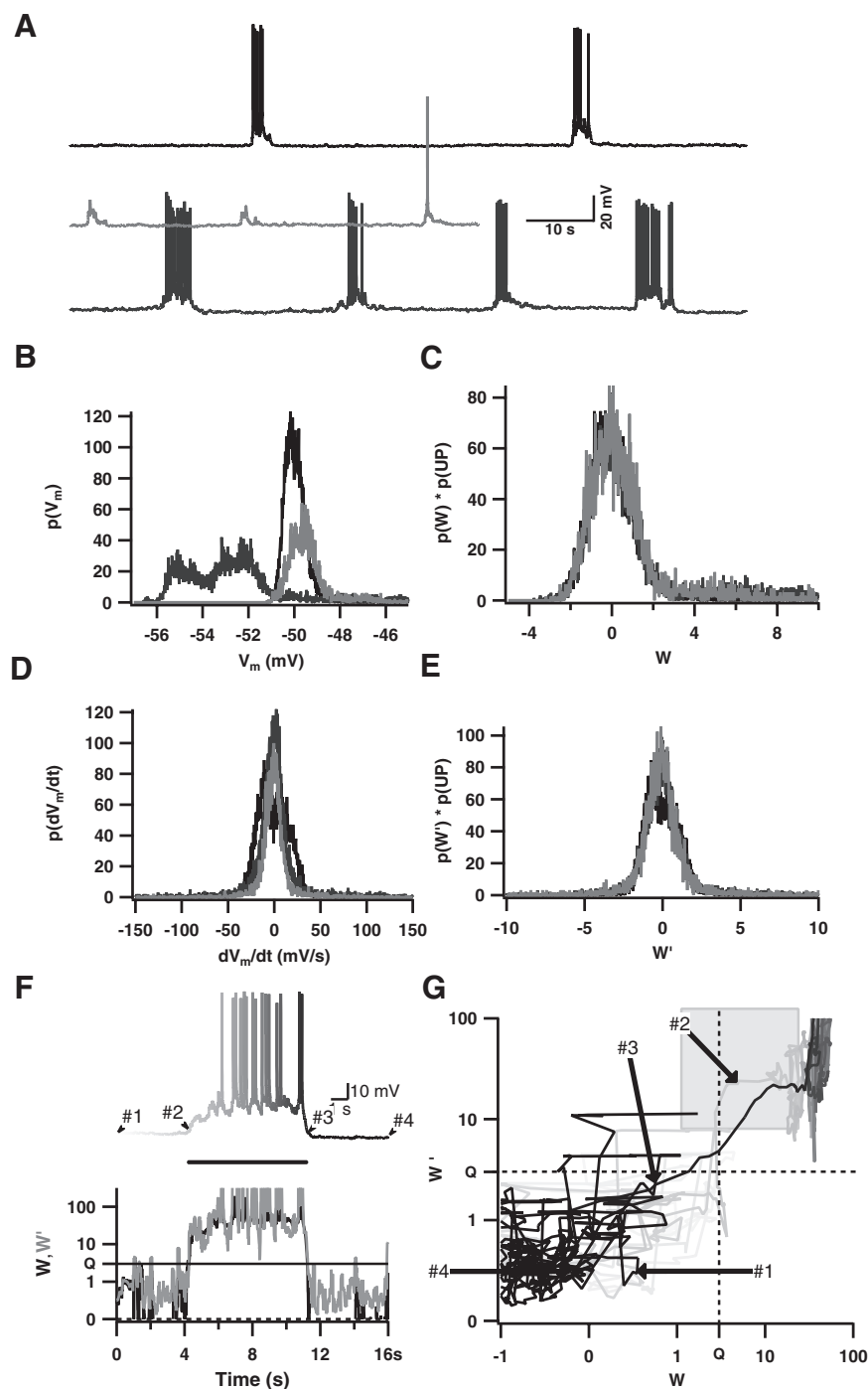


FIGURE 1. Discrimination of Up and Down states. **A**, Whole cell current clamp recordings from layer 2/3 pyramidal neurons in cortical slices taken from three different animals. The black and light-gray traces were recorded in neurons in a control slice; the dark gray trace was recorded from a neuron in a slice taken from a mouse 24 hours after chemoconvulsant-induced seizure. **B**, Histograms of the membrane potential (V_m) during a putative Down state for each of the three traces in (A). **C**, When the adaptive algorithm is applied, a transformation to the variable w (see Materials and Methods section) removes nonstationarity and normalizes each Down state to mean ~ 0 and variance ~ 1 . **D**, Same as (B), but for the first difference, dV_m/dt (at 100 Hz). **E**, Adaptive normalization for dV_m/dt , similar to (C). **F**, **Upper**: Membrane potential from a recording epoch, where numbers indicate a Down state (#1), the transition to the Up state (#2), the transition to the next Down state (#3), and the next-Down state (#4). The solid black bar indicates the region detected as the Up state by the adaptive algorithm. **Lower**: Time course for w (black, a transformation of V_m) and w' (gray, a transformation of dV_m/dt) during the recordings, illustrating a threshold Q that signals the onset ($w > Q$) and offset ($w < Q$) of an Up state. **G**, Trajectory of the recording in (F) through the (w, w') plane, coded in gray to match the timing in that recording.

RESULTS

Firing Rates Are Elevated After Seizure

To investigate changes in firing output of cortical circuits after prior seizure, we made intracellular recordings from layer 2/3 pyramidal neurons in somatosensory cortex 24 hours after chemoconvulsant injection. Analysis of firing output from layer 2/3 pyramidal neurons after seizure showed that spontaneous firing rates were doubled after a prior seizure episode (Fig. 2E; control: 0.12 ± 0.02 Hz, $n = 35$; postseizure:

0.22 ± 0.03 Hz, $n = 33$; $P < 0.005$; see also Shruti et al., 2008). Action potentials (APs) were almost exclusively discharged on an envelope of depolarization induced by a barrage of synaptic potentials. This brief period of network activation is characteristic of a cortical Up state (Sanchez-Vives and McCormick, 2000; Figs. 2A–2D). Synaptic events were also observed outside of these Up states (during Down states), although these rarely elicited an AP.

Up states lasted 1–10 seconds followed by Down states of 10- to 100-second duration (Figs. 2A–2D). On average, the frequency of Up

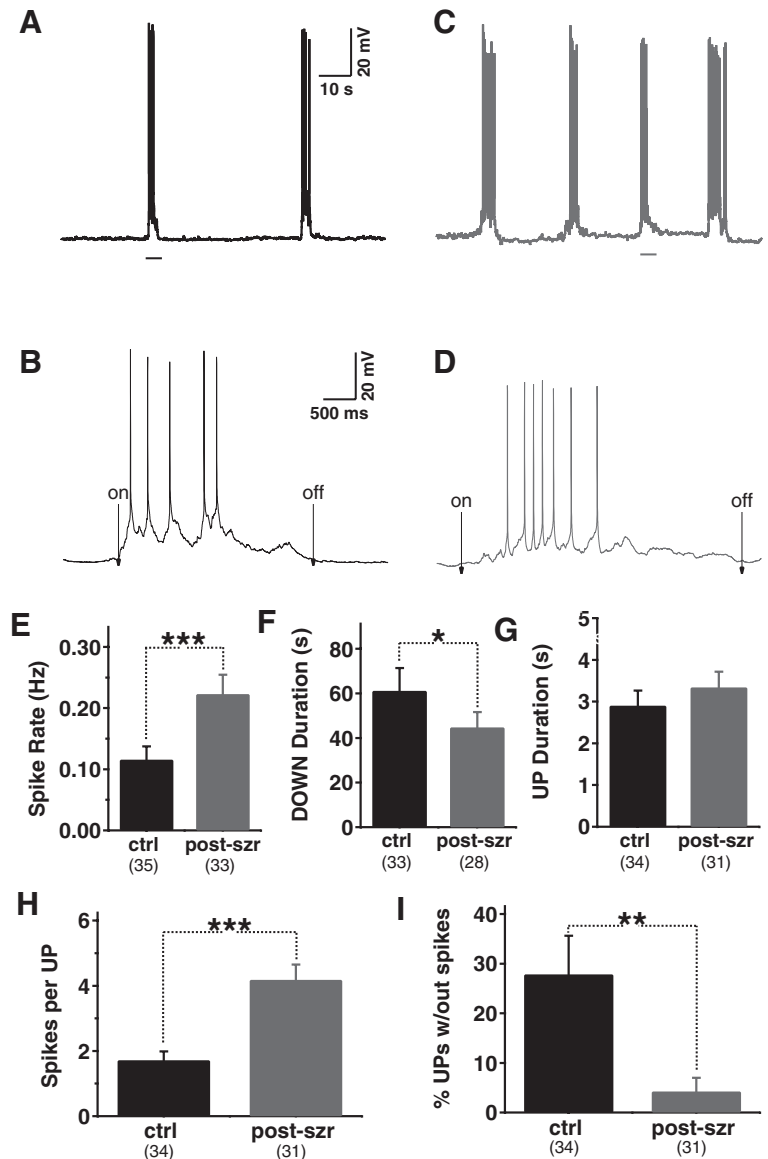


FIGURE 2. Spontaneous network activity is increased after epileptic seizure. **A**, Example of spontaneous firing activity recorded from a control cell. **B**, Expansion of the region underlined in **(A)**. **C**, Example recorded from a cell 24 hours after chemoconvulsant-induced seizure; scale as in **(A)**. **D**, Expansion of the region underlined in **(C)**; scale as in **(B)**. “On” marks Up state onset and “off” marks Down state onset as detected using the method shown in Fig. 1. **E**, The overall firing rate is higher in neurons from postseizure animals. **F**, Down state duration is decreased after seizure ($n =$ number of cells). **G**, Up states duration is not significantly changed. **H**, The total number of spikes per Up state is increased after seizure. **I**, The fraction of “spikeless” Up states is reduced nearly sevenfold after seizure.

states was significantly elevated in neurons from postseizure tissue (control: 0.016 ± 0.002 Hz, $n = 35$; postseizure: 0.026 ± 0.005 Hz, $n = 33$; $P < 0.005$). Correspondingly, the duration of Down states decreased from 61.2 ± 10.2 seconds to 44.8 ± 6.8 seconds (Fig. 2F, $P < 0.5$).

Up state duration was not enhanced after seizure (Fig. 2G; control: 2.91 ± 0.36 seconds; postseizure: 3.34 ± 0.38 seconds; $P > 0.4$), despite an increase in the number of APs that occurred during each Up state (Fig. 2H; control: 1.72 ± 0.27 ; postseizure: 4.18 ± 0.47 ; $P < 0.0001$). This suggests that cumulative firing output of layer 2/3 pyramidal neurons is not responsible for Up state termination. Overall, the increase in total AP output after seizure was due both to an increase in the frequency of Up states as well as an increase in the number of spikes per Up state.

Overall Increase in Spike Distribution Within Up States

Because Up state spike output was increased without an increase in Up state duration, it follows that the firing rate within an Up state is enhanced after seizure (control: 1.23 ± 0.09 Hz; postseizure: 1.71 ± 0.08 Hz; $P < 0.0001$). Where in the Up state are these extra spikes added? In control cells, many Up states contained no spikes (Fig. 2I;

27.9% of all Up states had no spikes), indicating that network Up states were sometimes insufficient to bring pyramidal neurons to threshold (see for example, Mukovski et al., 2006). After seizure, spikeless Up states were much less frequent (Fig. 2I; 4.2% with no spikes; $P < 0.0001$ vs. control), suggesting that neurons receive increased synaptic drive and/or exhibit enhanced intrinsic excitability after seizure. However, the increase in Up state firing output was not simply due to the conversion of spikeless Up states, since Up state firing rate was enhanced even when only Up states with at least one AP were examined (control: 1.58 ± 0.10 Hz; postseizure: 1.93 ± 0.07 Hz; $P < 0.005$). This analysis shows that the postseizure increase in Up state firing rate occurs by the addition of APs to both “subthreshold” and “suprathreshold” Up states.

Synaptic and Intrinsic Membrane Conductance Contributions to Increased Firing Rate

Postseizure firing output could be elevated because of altered synaptic activity and/or intrinsic properties of individual cells. It has been shown that seizures reduce synaptic inhibition and increase synaptic excitation (Hellier et al., 1999; Sutula et al., 1988; Wuarin

and Dudek, 2001). Indeed, membrane potential variance during Down states was elevated after prior seizure (control: 23.7 ± 1.4 mV/s; postseizure: 35.3 ± 1.9 mV/s; $P < 0.0001$), whereas membrane potential changes during Up states were difficult to assess because of the contribution of voltage-dependent conductances. To assess changes in synaptic input without contamination by such voltage-dependent conductances (including APs and subsequent after hyperpolarizations (AHPs)), experiments were performed in voltage clamp (Fig. 3A). Increased depolarizing membrane current, likely synaptic in origin, was observed during Up states (Figs. 3B–3F; control: 7.9 ± 0.6 pA; seizure: 17.7 ± 1.0 pA) and increased membrane current variance during Down states (Fig. 3G; control: 163.5 ± 5.1 pA/s; postseizure: 224.4 ± 8.2 pA/s; $P < 0.0001$) was observed in voltage clamp after seizure. The increased Down state variance did not seem to be due to an increase in nonspecific noise; rather, the frequency (but not amplitude) of spontaneous synaptic currents (both inhibitory and excitatory) was increased after seizure (data not shown). Thus, both increased variance and amplitude of current in Down and Up states, respectively, are likely to reflect increased activity in presynaptic populations, increasing both the instantaneous probability that an Up state will occur and that it will contain APs.

BK-Channel Antagonists Prevent Expression of the Postseizure Phenotype

We have previously shown that the activity of the large conductance potassium channel BK is upregulated after seizure (Shruti et al., 2008). Paxilline administration has a significant anticonvulsant effect *in vivo* (Sheehan et al., 2009) and normalizes both evoked and spontaneous firing rates to control levels in layer 2/3 neurons (Shruti et al., 2008). To understand how BK-channel antagonists influence cortical Up and Down states in both control and postseizure tissue, we applied the same analyses as in Fig. 2.

Increased firing rates after seizure were reversed by BK-channel antagonists (Fig. 4A; see also Shruti et al., 2008). Although antagonist-mediated reduction in overall firing rates was also observed in controls, the magnitude of the decrease was larger in postseizure tissue. Antagonist-induced reductions in overall firing rates were largely due to a decrease in the firing rates with Up states (Fig. 4B) rather than a reduction in the duration or rate of Up states (Figs. 4C–4F). The fraction of Up states containing no APs at all was dramatically increased by BK-channel antagonists (Fig. 4G), and the Down state variance was decreased (Fig. 4H). These results suggest that the forces initiating network Up states are intact under BK-channel antagonism—even in highly excitable postseizure tissue. However, neural firing output in layer 2/3 pyramidal cells, a product of synaptic input and intrinsic excitability, is suppressed after antagonist administration. Because BK-channel antagonists can reduce firing output in a cell-autonomous manner (Shruti et al., 2008), it is reasonable to hypothesize that blocking BK channels reduces Up state firing activity by specifically suppressing spike output of layer 2/3 neurons.

DISCUSSION

We have developed a quantitative, automated method for identifying Up and Down state transitions during spontaneous neuronal firing *in vitro*, using cell-specific criteria based on membrane potential mean and variance as they evolve over time. We have used this method to evaluate how prior seizures change spontaneous firing activity, as well as how the anticonvulsant effect of BK-channel antagonists is manifested in neocortical networks. The homeostatic hypothesis predicts that increased activity history should downregulate network activity. Consistent with this hypothesis, mild-patterned stimulation in developing organotypic cortical

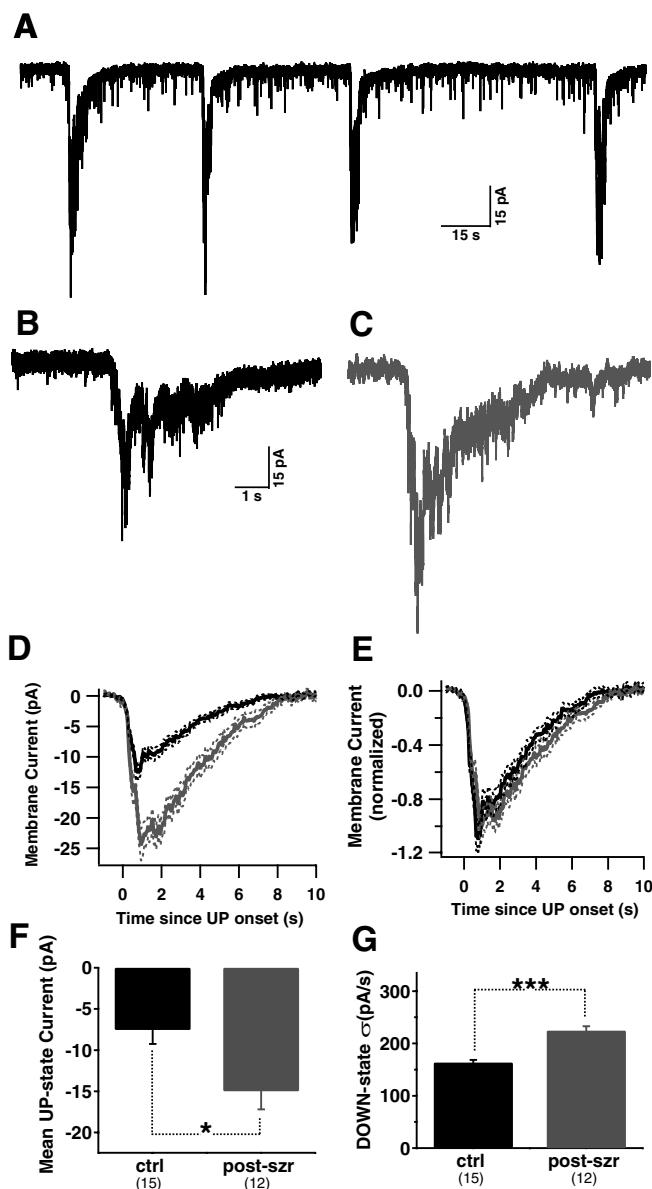


FIGURE 3. Increased membrane currents during both Up and Down states after seizure. **A**, Voltage clamp recording from a control layer 2/3 pyramidal neuron across four Up states. Example of membrane current during an Up state in **(B)** a control neuron and **(C)** a neuron recorded 24 hours after chemoconvulsant-induced seizure. Scale as in **(B)**. **D**, Mean membrane current (averaged across Up states; Up states terminating before the longest Up state contribute zero to the mean) is greater throughout the Up state in postseizure neurons. Dotted lines indicate standard error. **E**, Both conditions show a similar time course of current, after peak normalization to scale the averaged traces. **F**, Summary of **(D)**. **G**, Standard deviation of smoothed, differentiated Down state membrane current shows that Down states show significantly greater fluctuations in membrane current after seizure.

cultures produces a downregulation of Up state activity (Johnson and Buonomano, 2007). However, in response to a history of abnormal and elevated activity produced by seizure *in vivo*, we find

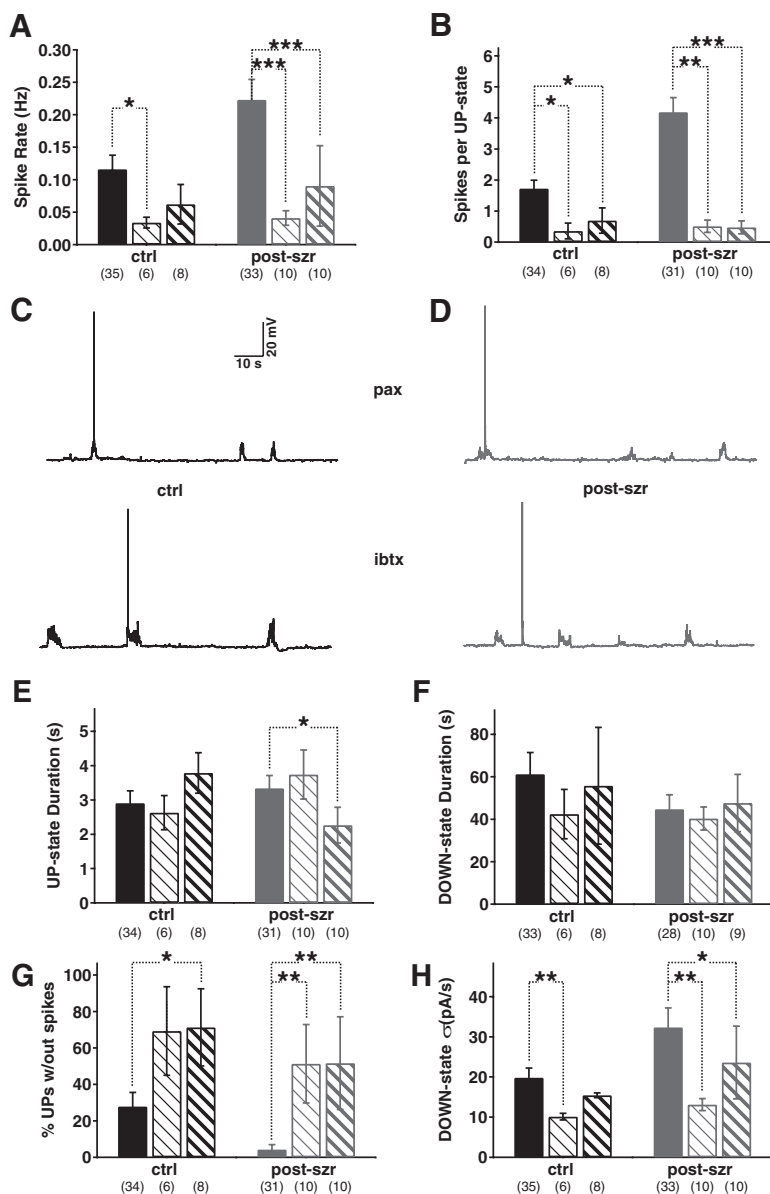


FIGURE 4. BK-channel antagonists suppress Up state firing but not network activity. **A**, Paxilline (10 nM; light hatch in all panels) or iberiotoxin (50 nM; heavy hatch in all panels) reduce firing rates to similar levels in control and postseizure neurons. Control data is replotted from Fig. 2A. **B**, Antagonist-mediated firing rate reduction can be attributed to reduced firing during Up states. **C**, Membrane potential recording of control neurons in the presence of either paxilline (pax; upper panel) or iberiotoxin (ibtx; lower panel). **D**, Same as (C), but for postseizure neurons. **E**, Up state duration is typically not affected by either paxilline or iberiotoxin, and (F) duration of Down states is also unaltered. **G**, The fraction of “spikeless” Up states is significantly increased by BK-channel antagonists, reaching similar levels in both control and postseizure neurons. **H**, Down state membrane potential variability is reduced to similar levels in the two experimental conditions.

that firing rates become elevated because of an increase in Up state frequency and Up state firing rate. Although increased membrane potential variance near *in vivo* resting potentials may contribute to this increase in firing output, previous studies have established that a postseizure gain-of-function in BK channel currents is associated with a cell-autonomous increase in firing output.

Synaptic Noise and Increases in Neuronal Gain

We found that both Up state firing rate and Down state membrane potential noise are elevated after seizure. Analysis of spontaneous synaptic activity during both Up and Down states revealed an increase in the frequency of depolarizing synaptic events. Because other investigations have shown that synaptic noise can lead to a multiplicative increase in spike output (Chance et al., 2002; Higgs et al., 2006; Ho and Destexhe, 2000), it is reasonable to conclude that this is at least a partial explanation for the postseizure increase in firing activity. An increase in Down state noise (because of increases in background synaptic activity or fluctuations in leak

channel currents) could increase the probability of firing within the network, facilitating the transition to an Up state and increasing the frequency of Up states. Although it is unlikely that an increase in noise is solely responsible for the postseizure increase in firing rates described here—indeed, a postseizure change in a number of ionic conductances and intrinsic excitability has been well characterized (Bernard et al., 2004; Chen et al., 2001; Shah et al., 2004; Su et al., 2002)—these results are highly consistent with a number of *in vitro* and *in silico* studies (Chance et al., 2002; Higgs et al., 2006).

Up State Duration Is Fixed Despite Increased Firing Output

Because layer 2/3 neurons are densely interconnected, it is reasonable to expect that increased Up state firing rates would extend Up state duration as recurrent excitation propagated through the cortical network (eg, see Holcman and Tsodyks, 2006). However, we did not find this to be the case (Fig. 2G; also in voltage

clamp recordings: control: 3.17 ± 0.19 seconds vs. postseizure: 3.42 ± 0.23 seconds; $P > 0.3$). This may suggest that Up state termination is due to the activity of a separate cell population, such as a subset of interneurons, and that the balance between excitation and inhibition is maintained in a cortical network (Shu et al., 2003). Alternatively, Up state duration may be controlled by a limited supply of presynaptic glutamate (Staley et al., 1998). Another possibility is that activation of cell-autonomous hyperpolarizing conductances, activated by sustained low-threshold depolarization during the Up state, may suppress firing and terminate the Up state. Resolution of these issues will require a more extensive analysis of cellular and circuit-level changes in neocortical columns.

Consequences of Increased Up State Activity

Seizure history has been shown to interfere with short-term memory formation (Kim and Routtenberg, 1976), and it is tempting to speculate that this interference occurs in part because abnormal Up state activity degrades the stability of specific synaptic changes that may underlie memory formation. Although it is not known whether the alterations in Up state activity are sustained, as this analysis was restricted to a 24-hour period after chemoconvulsant-induced seizures, it is conceivable that the changes observed may have long-term consequences for brain function. Because recurrent network activity may serve to consolidate synaptic connections between neurons (Hebb, 1949), increased Up state activity might induce synaptic consolidation of pathologic circuits to promote the generation of future seizures. In addition, activity-dependent changes in ion channel expression may also alter input-output transformations at the level of an individual neuron. Thus, increased activity may under some circumstances be pathologically reinforcing.

Seizure history is a strong predictor for future seizure susceptibility (Elwes et al., 1985)—even in animal models without an underlying genetic susceptibility—although it remains controversial whether the putative reorganization of brain circuits as a result of seizures themselves is itself an aggravating factor. These data suggest that reducing postseizure abnormal activity might be a useful clinical goal in preventing epileptogenesis (Kadam et al., 2010; Williams et al., 2009) and indicate that BK-channel antagonists may be useful therapeutic agents.

Methodological Advances and Alternative State Detection Methods

A simple fixed threshold has been used by numerous investigators to classify states in intracellular recordings. One standard is to place this threshold at a fixed distance between the Up and Down state peaks in a membrane potential histogram constructed *post hoc* (Anderson et al., 2000; Hasenstaub et al., 2007; Metherate and Ashe, 1993; Reynolds and Wickens, 2003; Sanchez-Vives and McCormick, 2000). More sophisticated methods involve using the intersection times of a narrow-window and a wide-window running mean to identify state transitions (Seamari et al., 2007) or using both the membrane potential mean and variance and segregating according to a fixed threshold in a two-dimensional space (Frohlich et al., 2006). All of these approaches are limited theoretically and practically because (a) they assume stationarity in the data, (b) they fail to account for inhomogeneity in the membrane potential variance, and thus, the probability of spurious threshold crossings, (c) they require computation of thresholds *post hoc* rather than online, (d) the value of the threshold chosen does not have any simple mathematical relation to the likelihood that it will be crossed, or (e) any or all of the above. By contrast, the method presented here adapts automatically to multiple local statistics of the data, variations of which could reflect variability in input resistance, spontaneous synaptic input, electrode access resistance within and across recordings. It is

this automatic adaptation that distinguishes and improves on previous attempts to identify state transitions in intracellular recordings. As a further direction, one might construct a hidden Markov model that would use both the membrane potential mean and variance to classify network states; such a model might work at least as well as the one described here. However, such a method would also be complicated by nonstationarity in the data and likely be computationally intensive. The adaptive threshold method, however, is both computationally inexpensive and easy to implement. A performance comparison of our adaptive threshold method to other methods, using both simulated data and “manual” analysis of experimental data, is available on request and will be presented in a forthcoming manuscript (R.C.G., A.L.B., and R.E.K.).

ACKNOWLEDGMENT

The authors thank Erika Fanselow for critical comments on the manuscript.

REFERENCES

- Abegg MH, Savic N, Ehrenguber MU, et al. Epileptiform activity in rat hippocampus strengthens excitatory synapses. *J Physiol*. 2004;554:439–448.
- Anderson J, Lampl I, Reichova I, et al. Stimulus dependence of two-state fluctuations of membrane potential in cat visual cortex. *Nat Neurosci*. 2000;3:617–621.
- Bains JS, Longacher JM, Staley KJ. Reciprocal interactions between CA3 network activity and strength of recurrent collateral synapses. *Nat Neurosci*. 1999;2:720–726.
- Beenhakker MP, Huguenard JR. Neurons that fire together also conspire together: is normal sleep circuitry hijacked to generate epilepsy? *Neuron*. 2009;62:612–632.
- Bernard C, Anderson A, Becker A, et al. Acquired dendritic channelopathy in temporal lobe epilepsy. *Science*. 2004;305:532–535.
- Chagnac-Amitai Y, Connors BW. Horizontal spread of synchronized activity in neocortex and its control by GABA-mediated inhibition. *J Neurophysiol*. 1989;61:747–758.
- Chance FS, Abbott LF, Reyes AD. Gain modulation from background synaptic input. *Neuron*. 2002;35:773–782.
- Chen K, Aradi I, Thon N, et al. Persistently modified h-channels after complex febrile seizures convert the seizure-induced enhancement of inhibition to hyperexcitability. *Nat Med*. 2001;7:331–337.
- Echevarria D, Albus K. Activity-dependent development of spontaneous bioelectric activity in organotypic cultures of rat occipital cortex. *Brain Res Dev Brain Res*. 2000;123:151–164.
- Elwes RD, Chesterman P, Reynolds EH. Prognosis after a first untreated tonic-clonic seizure. *Lancet*. 1985;2:752–753.
- Fishman RA. *Cerebrospinal Fluid in Diseases of the Nervous System*. 2nd ed. Philadelphia, PA: Elsevier Health Sciences; 1992.
- Frohlich F, Bazhenov M, Timofeev I, et al. Slow state transitions of sustained neural oscillations by activity-dependent modulation of intrinsic excitability. *J Neurosci*. 2006;26:6153–6162.
- Haider B, McCormick DA. Rapid neocortical dynamics: cellular and network mechanisms. *Neuron*. 2009;62:171–189.
- Hasenstaub A, Sachdev RN, McCormick DA. State changes rapidly modulate cortical neuronal responsiveness. *J Neurosci*. 2007;27:9607–9622.
- Hebb DO. *The Organization of Behavior*. New York: Wiley; 1949.
- Hellier JL, Patrylo PR, Dou P, et al. Assessment of inhibition and epileptiform activity in the septal dentate gyrus of freely behaving rats during the first week after kainate treatment. *J Neurosci*. 1999;19:10053–10064.
- Higgs MH, Slee SJ, Spain WJ. Diversity of gain modulation by noise in neocortical neurons: regulation by the slow afterhyperpolarization conductance. *J Neurosci*. 2006;26:8787–8799.
- Ho N, Destexhe A. Synaptic background activity enhances the responsiveness of neocortical pyramidal neurons. *J Neurophysiol*. 2000;84:1488–1496.
- Holcman D, Tsodyks M. The emergence of Up and Down states in cortical networks. *PLoS Comput Biol*. 2006;2:e23.
- Jensen FE. Epileptogenic cortical dysplasia: emerging trends in diagnosis, treatment, and pathogenesis. *Epilepsia*. 2009;50 Suppl 9:1–2.
- Johnson HA, Buonanno DV. Development and plasticity of spontaneous activity and Up states in cortical organotypic slices. *J Neurosci*. 2007;27:5915–5925.
- Kadam SD, White AM, Staley KJ, Dudek FE. Continuous electroencephalographic monitoring with radio-telemetry in a rat model of perinatal hypoxia-ischemia reveals progressive post-stroke epilepsy. *J Neurosci*. 2010;30:404–415.

- Kim HJ, Routtenberg A. Retention disruption following post-trial picrotoxin injection into the substantia nigra. *Brain Res.* 1976;113:620–625.
- Maffei A, Nelson SB, Turrigiano GG. Selective reconfiguration of layer 4 visual cortical circuitry by visual deprivation. *Nat Neurosci.* 2004;7:1353–1359.
- Metherate R, Ashe JH. Ionic flux contributions to neocortical slow waves and nucleus basalis-mediated activation: whole-cell recordings in vivo. *J Neurosci.* 1993;13:5312–5323.
- Mukovski M, Chauvette S, Timofeev I, Volgushev M. Detection of active and silent states in neocortical neurons from the field potential signal during slow-wave sleep. *Cereb Cortex.* 2007;17:400–414.
- Petersen CC, Hahn TT, Mehta M, et al. Interaction of sensory responses with spontaneous depolarization in layer 2/3 barrel cortex. *Proc Natl Acad Sci USA.* 2003;100:13638–13643.
- Reynolds JN, Wickens JR. A state-dependent trigger for electrophysiological recording at predetermined membrane potentials. *J Neurosci Methods.* 2003;131:111–119.
- Sanchez-Vives MV, McCormick DA. Cellular and network mechanisms of rhythmic recurrent activity in neocortex. *Nat Neurosci.* 2000;3:1027–1034.
- Seamari Y, Narváez JA, Vico FJ, et al. Robust off- and online separation of intracellularly recorded up and down cortical states. *PLoS One.* 2007;2:e888.
- Shah MM, Anderson AE, Leung V, et al. Seizure-induced plasticity of h channels in entorhinal cortical layer III pyramidal neurons. *Neuron.* 2004;44:495–508.
- Shao LR, Dudek FE. Increased excitatory synaptic activity and local connectivity of hippocampal CA1 pyramidal cells in rats with kainate-induced epilepsy. *J Neurophysiol.* 2004;92:1366–1373.
- Sheehan JJ, Benedetti BL, Barth AL. Anticonvulsant effects of the BK-channel antagonist paxilline. *Epilepsia.* 2009;50:711–720.
- Shruti S, Clem RL, Barth AL. A seizure-induced gain-of-function in BK channels is associated with elevated firing activity in neocortical pyramidal neurons. *Neurobiol Dis.* 2008;30:323–330.
- Shu Y, Hasenstaub A, McCormick DA. Turning on and off recurrent balanced cortical activity. *Nature.* 2003;423:288–293.
- Staley KJ, Longacher M, Bains JS, Yee A. Presynaptic modulation of CA3 network activity. *Nat Neurosci.* 1998;1:201–209.
- Steriade M, Amzica F. Sleep oscillations developing into seizures in corticothalamic systems. *Epilepsia.* 2003;44 Suppl 12:9–20.
- Steriade M, Nunez A, Amzica F. A novel slow (<1 Hz) oscillation of neocortical neurons in vivo: depolarizing and hyperpolarizing components. *J Neurosci.* 1993;13:3252–3265.
- Su H, Sochivko D, Becker A, et al. Upregulation of a T-type Ca²⁺ channel causes a long-lasting modification of neuronal firing mode after status epilepticus. *J Neurosci.* 2002;22:3645–3655.
- Sutula T, He XX, Cavazos J, Scott G. Synaptic reorganization in the hippocampus induced by abnormal functional activity. *Science.* 1988;239:1147–1150.
- Takada H, Aso K, Watanabe K, et al. Epileptic seizures induced by animated cartoon, “Pocket Monster.” *Epilepsia.* 1999;40:997–1002.
- Tsau Y, Guan L, Wu JY. Epileptiform activity can be initiated in various neocortical layers: an optical imaging study. *J Neurophysiol.* 1999;82:1965–1973.
- Williams PA, White AM, Clark S, et al. Development of spontaneous recurrent seizures after kainate-induced status epilepticus. *J Neurosci.* 2009;29:2103–2112.
- Willoughby JO, Mackenzie L, Medvedev A, Hiscock JJ. Distribution of Fos-positive neurons in cortical and subcortical structures after picrotoxin-induced convulsions varies with seizure type. *Brain Res.* 1995;683:73–87.
- Wuarin JP, Dudek FE. Excitatory synaptic input to granule cells increases with time after kainate treatment. *J Neurophysiol.* 2001;85:1067–1077.
- Zou Q, Rudolph M, Roy N, et al. Reconstructing synaptic background activity from conductance measurements in vivo. *Neurocomputing.* 2005;65–66: 673–678.